Available online at www.sciencedirect.com
SCIENCE DIRECT®
Journal of Catalysis 221 (2004) 325–334
JOURNAL OF CATALYSIS
www.elsevier.com/locate/jcat

Study of nickel catalysts supported on silica of low surface area and prepared by reduction of nickel acetate in aqueous hydrazine

A.G. Boudjahem, S. Monteverdi, M. Mercy, and M.M. Bettahar *

Laboratoire de Catalyse Hétérogène, UMR CNRS 7565, Faculté des Sciences, Université Henri Poincaré, Nancy-I, BP 239, 54506 Vandœuvre cédex, France

Received 23 May 2003; revised 4 August 2003; accepted 4 August 2003

Abstract

Nickel metal nanoparticles supported on low surface area silica were prepared by reduction of nickel acetate with hydrazine in aqueous medium. The catalysts were characterized by atomic absorption, XRD, TEM, BET surface area, and H_2 chemisorption and TPD. Their hydrogenating properties were evaluated in the gas-phase hydrogenation of benzene. It was found that gas-phase stability and surface properties of the supported nickel particles depended on the nature and temperature of pretreatment. Small nickel particles, in an oxidized or reduced state, were strongly resistant to reducing or oxidizing treatment, respectively. For H_2-treated catalysts, H_2 chemisorption and TPD results suggested the occurrence of hydrogen spillover between the metal nickel phase and the silica. For air and H_2-treated catalysts, hydrogen spillover seemed to involve, in addition, the NiO phase. The activity of the catalysts in benzene hydrogenation also depended on the thermal pretreatment. Precalcined and then reduced catalysts exhibited higher TOFs than nonprecalcined catalysts, suggesting that the presence of the NiO phase may have influenced the hydrogenation process. A comparative study showed that a catalyst prepared by reduction of nickel acetate by hydrazine in aqueous medium stored more hydrogen and was more active in benzene hydrogenation than a conventional catalyst.

Keywords: Nickel catalysts; Nanoparticles; Silica; Hydrazine; Hydrogen chemisorption and TPD; Benzene hydrogenation

1. Introduction

Conventional supported metal catalysts are prepared by in situ reduction of a metal salt. The catalytic activity of the metal particles is strongly influenced by their size and shape [1–6]. However, it is often difficult to control the morphology of the final material, notably for impregnated catalysts [1–10]. An alternative method for obtaining supported catalysts with well-defined metal particles is the preparation of supported catalysts from metal colloids.

Metal nanoparticle research has recently become the focus of intense work due to their unusual properties compared to bulk metal. The reason for such avid research arises from the drastic increase of the surface to volume ratio to such an extent that the material properties are determined much more by the surface atoms than by the framework atoms, with the result that the physical and chemical properties of the particles differ considerably from those of bulk solids [11–16]. They hold promise for use as advanced materials for electronic, magnetic, optical, and thermal properties [17,18] and have also been applied in heterogeneous catalysis [15,19–25]. The chemical route for the preparation of such materials is of particular interest since it allows a better control of the structure at the microscopic level [26–38]. The chemical methods have generally involved the reduction of the relevant metal salt in the presence of a stabilizer such as linear polymers [14,39–42], ligands [42,43], surfactants [38,44–46], tetraalkylammonium salts [47,48], or heterogeneous supports [49–51] which prevent the nanoparticles from agglomerating.

Previous work of our group showed that supported nickel nanoparticles can be obtained in organic medium by reducing nickel acetate by NaH in the presence of an alcoholate surfactant [24,25]. They were found to be active catalysts in the gas-phase hydrogenation of benzene after thermal pretreatment. The stability and activity of the nanoparticles depended on the nature of the pretreatment and nickel loading.

Recent works have pointed out the interest of working in aqueous medium as a practical solution for the future in homogeneous and heterogeneous catalysis [52]. This prompted

* Corresponding author.
E-mail address: mohammed.bettahar@lcah.u-nancy.fr (M.M. Bettahar).

0021-9517/$ – see front matter © 2003 Published by Elsevier Inc.
doi:10.1016/j.jcat.2003.08.002

us to undertake a study of nickel nanoparticles obtained by reduction of nickel salts in aqueous medium and stabilized on a silica support of low surface area. The surface properties of the obtained catalysts were tested in gas-phase hydrogenation of benzene.

Despite of the high number of studies published in the past decades, increasing attention is paid to the hydrogenation of aromatics because of the stringent environmental regulations governing their concentration in diesel fuels [53–56]. Benzene hydrogenation has been chosen as the model aromatic feedstock [57,58]. This reaction has also been used as a model reaction in heterogeneous catalysis by metals where metal–support interactions are involved [56–60]. Hydrazine was used because recent studies showed that it is a good reducing agent in aqueous medium for noble and transition metals ions [51,61–63]. As to the silica support, it is known not to give rise to nickel mixed oxides and to allow a better approach of the particle size effect in the behavior of supported nickel catalysts. Moreover, generally speaking, nickel-supported catalysts have been concerned with high surface area supports and nickel loadings higher than 5 wt%. Also the use of silica of low surface area and low nickel loading in the preparation of nickel-based catalysts was expected to give rise to an important contribution to the existing corpus of literature on Ni/SiO_2 systems [7]. We were also encouraged in this way because preliminary results showed that, in aqueous medium, the nickel reduction process was enhanced in the presence of low surface area silica, whereas silica of high surface area tended to inhibit it.

The present study reports the results obtained over nickel (1–5 wt%) supported on silica of low area (15 $m^2\,g^{-1}$) prepared by reduction of nickel acetate with hydrazine in aqueous medium. The stability and surface properties of the nickel particles were examined under hydrogen or air atmosphere and correlated to their catalytic activity in benzene hydrogenation. The catalysts were characterized by XRD, TEM, and hydrogen chemisorption and TPD. For comparison, a classical catalyst, prepared by impregnating the same silica support with nickel acetate, was also studied.

2. Experimental

2.1. Catalyst preparation

Doubly distilled water was used as a solvent. Nickel acetate tetrahydrate ($\geqslant$99.0%, Fluka) and aqueous hydrazine 24–26% ($\geqslant$99.0%, Fluka) were used as received. The silica support (Chempur, 99.99%, 15 $m^2\,g^{-1}$ and grains of 325 mesh) was pretreated in air at 500 °C for 10 h with a heating rate of 10 °C min^{-1} and stored under argon.

The silica support (3.0–4.0 g) was impregnated with 25 mL of aqueous solution of nickel acetate. The nickel acetate concentration in the solution was calculated to obtain the nominal composition of 1.0–5.0 wt% Ni. The suspension was stirred for 16 h at room temperature. The solvent was then evaporated at 80 °C under vacuum, and the obtained solid was dried for 16 h at 100 °C.

Table 1
Ni content and particle size of the catalysts

Catalyst	Ni (%)	Treatment	Particle size (nm)		
			XRD	TEM	H_2 chem
AB11	0.86	None	5.5	–	–
		H_2/300 °C/2 h	–	∼4	5.5
AB12	1.40	None	5.7	–	–
		H_2/300 °C/2 h	–	–	14.8
AB32	2.73	None	11.8	–	–
		H_2/300 °C/2 h	16.6	∼14	30.0
		Air/250 °C/2 h	8.3	–	–
		Air/250 °C/2 h then H_2/300 °C/2 h	–	–	28.4
AB53	4.30	None	13.8	–	–
		H_2/300 °C/2 h	24.7	∼15	32.8
AC30	4.50	H_2/300 °C/2 h	–	–	28.9

The preparation of the supported reduced nickel particles was performed under argon atmosphere in a 3-necked reaction flask of 500 mL dipping in an oil bath. The reaction flask was fitted with a reflux condenser and a thermocouple for the control of the reaction temperature. The supported nickel acetate precursor was introduced in the reaction flask filled with 120 mL of bidistilled water. The suspension was stirred for 20 min at room temperature and then 10 mL of hydrazine solution (in excess) was added. The pH of the solution was 10–12 and remained almost constant during the reduction process. The reaction mixture was slowly heated from room temperature to 80 °C. The suspension became translucent as the reaction temperature was raised and turned to a black color at 80 °C. The black suspension was maintained at this temperature for 30 min and cooled at room temperature. It was filtered and washed several times with water until neutral pH was obtained. The filtrate was dried at 60 °C under vacuum. The resulting solid was stored under argon. The catalysts were denoted as AB11, AB12, AB32, and AB53 (for corresponding nickel content, see Table 1).

The classical supported catalyst, denoted as AC30, was prepared by calcinating the supported nickel acetate in air at 300 °C for 2 h. The nickel oxide obtained was pretreated under hydrogen at 300 or 400 °C for 1 h before the chemisorption or testing studies.

2.2. Equipment

The nickel content and specific surface area of the catalysts were determined on a Varian AA1275 atomic absorption spectrophotometer and Carlo Erba Sorptomatic 1900 equipment, respectively. The electron microscopy images were obtained with a Phillips CM20 STEM after placing a drop of the nanoparticle suspension on the carbon-

coated copper grid. XRD patterns were recorded with a classical $\theta/2\theta$ diffractometer using Cu-K_α radiation.

Chemisorption and thermal treatments experiments were carried out in a pulse chromatographic microreactor. The reactor was equipped with the catharometric detector of a microchromatograph (AT M200, Hewlett Packard) fitted with molecular sieve columns and MTI software.

The gas-phase hydrogenation reaction was carried out in a fixed-bed quartz reactor. The reactant and product analyses were conducted on line in a Hewlett Packard 5730A FID gas chromatograph. Benzene, cyclohexane, cyclohexene, and methylcyclopentane were analyzed with TCEP (2 m, 1/8 inch) and Sterling (3 m, 1/8 inch) columns, respectively. A Kontron software was utilized for data processing.

2.3. Chemisorption and thermal treatments

The chemisorption, thermodesorption, and hydrotreatment were carried out over 0.1 g samples. The gases were purchased from Air Liquide. Oxygen traces were eliminated from argon (99.995%) and hydrogen (99.995%) by using a manganese oxytrap (Engelhardt) whereas helium (99.999%), air, and oxygen diluted in argon were used as received.

For the non calcined catalysts, the fresh sample was heated under a stream of pure H_2 (50 mL min^{-1}) at 300, 400, and 500 °C with a heating rate of 10 °C min^{-1}. The sample was maintained at each of these temperatures for 2 h and purged under an argon flow (100 mL min^{-1}) at the same temperature for 2 h. After this purging time no hydrogen (<1 ppm v/v) was detected in the exit gases. For the chemisorption studies, the pretreated catalyst was cooled at room temperature under argon atmosphere and the reactant gas (100 ppm H_2/argon or 150 ppm O_2/helium) was injected in the reactor every 2 min. The subsequent hydrogen TPD was conducted after purging the sample under argon then flowing the same gas (50 mL min^{-1}) in programmed temperature mode up to 700 °C using a ramp of 7.5 °C min^{-1}.

For the calcined catalysts, the fresh sample was treated under a stream of 50 mL min^{-1} of air with a heating rate 7.5 °C min^{-1} up to 250 or 300 °C. The sample was maintained at this temperature for 2 h, rapidly cooled at room temperature under flowing argon, and purged for 2 h. The calcined catalyst obtained was subsequently reduced under pure H_2 and chemisorption and TPD studies were conducted as described above for the noncalcined catalyst.

Assuming spherical metal particles, the mean size was calculated from the following relation [3]: $d = 971/D$, where D is the metal dispersion.

2.4. Catalyst testing

The catalytic experiments were carried out over 0.05 g of catalyst under a total flow of 50 cm^3 min^{-1} under atmospheric pressure and in the temperature range 75–225 °C. The reaction temperature was varied by the crossing method as follows: 75, 100, 150, 200, 225, 175, 125, and 75 °C. Each reaction temperature was maintained constant until the steady state was reached, as indicated by gas chromatography analysis of the exit gases.

The reactant feed gas was obtained by flowing H_2 in benzene (Merck, 99.5%) placed in a saturator maintained at 5.3 °C in order to obtain a mixture of 1% benzene diluted in hydrogen.

3. Results and discussion

The results of the reduction of supported nickel acetate by aqueous hydrazine showed that the surface and catalytic properties of the nickel nanoparticles depended on several factors: concentration of the nickel salt and hydrazine, pH of the solution, temperature and time of reduction, and nature of the support. In the case of silica support, it was found that the reduction process was enhanced by a low surface area material, and inhibited by a high surface area material. In the present study, results obtained over catalysts with various metal loadings prepared at 80 °C using a low surface area silica as support (15 m^2 g^{-1}) are reported. For comparison, a conventional catalyst prepared with the same precursor and support was also studied. Results on the factors governing the reducibility of nickel acetate by aqueous hydrazine will be reported in a separate publication.

3.1. Characterization

The XRD spectrum showed crystallized silica. That of the fresh catalysts exhibited a main and large reflection at 44.5° 2θ characteristic of metallic nickel with a *cfc* structure. A typical spectrum is illustrated in Fig. 1. However, samples AB32 and AB53 also presented the reflection of $Ni(OH)_2$ at 38.5° 2θ with a *hcp* structure. This result is in agreement with recent literature data showing that, in alkaline medium,

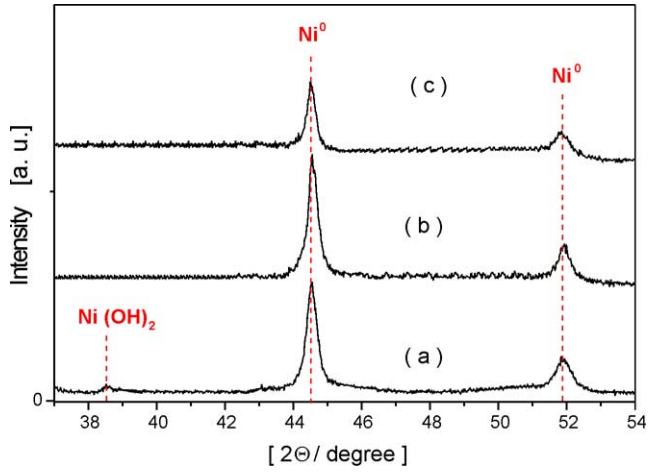

Fig. 1. XRD pattern of AB32 catalyst. Effect of the pretreatment: (a) none; (b) H_2/300 °C/2 h; (c) air/250 °C/2 h.

nickel sulfate formed the $[Ni(N_2H_4)_3]^{2+}$ complex with hydrazine at room temperature, which decomposed to pure Ni^0 or a mixture of Ni^0 and $Ni(OH)_2$ according to the temperature and pH of the reaction medium [62].

The mean size of the fresh particles, estimated using the Debye–Scherrer equation, was dependent on the nickel loading. The higher the nickel loading, the higher the particle size (Table 1): for nickel contents increasing from 1 to 5%, the mean particle size increased from about 5 to 14 nm. At high nickel loading, part of the precursor would not directly, or less directly, interact with the support and probably migrate more easily, accounting for the bigger average particle size during the aqueous hydrazine reduction process. In contrast, at lower nickel contents, the metal particles being stabilized by the support would be less prone to coalescence.

After treatment under hydrogen at 300 °C, the catalysts only exhibited the characteristic reflection of metallic nickel, as shown in Fig. 1. The AB32 and AB53 catalysts were sensitive to the thermal treatment under H_2, which increased the nickel particle size from 11.8 to 16.6 nm, and from 13.8 to 24.7 nm, respectively. Under such conditions, the metal nickel particles coalesced through diffusion at the support surface. Such a mechanism probably holds for those particles in weaker interaction with the support.

The growth of the particle size can also be related to the thermal decomposition of the organic matrix under hydrogen atmosphere at 300 °C. Indeed, for all the catalysts, the treatment under H_2 in temperature-programmed mode led to the formation of methane and, to some extent, of carbon monoxide. In addition, molecular hydrogen was formed when the fresh samples were treated under a flow of argon instead of hydrogen. These molecules resulted from the decomposition of the acetate fragment of the catalyst precursor. The presence of organic fragments in the reduced final material indicated that they were still attached—at least partly—to the nickel phase, playing the role of a stabilizing agent [24,25].

The fresh samples calcined in air at 250 °C, strikingly, did not exhibit the characteristic reflection of NiO but of metallic nickel (Fig. 1). Moreover, the mean particle size of the metallic phase decreased to 8.0 nm. The persistence of the Ni^0 diffraction peak was ascribed to the presence of small metal aggregates in the fresh particles which were resistant to oxidation under air at 250 °C, presumably because of the existence of chemical interactions with the support or of a low rate of nucleation during the oxidation process. Larger particles were more easily oxidized to NiO. The absence of the characteristic reflection of this phase suggests a high dispersion on the silica support: the oxide particles formed were probably attached to the support by strong Ni^{2+}–O bonds, and thus less prone to sintering during the thermal oxidizing treatment. The influence of an oxygen thermal treatment on the dispersion of metallic nickel has been reported [64].

The TEM study indicated that after hydrogen treatment at 300 °C, the metal nanoparticles were homogeneously dispersed on the support (Fig. 2). The average particle size was about 4, 14, and 15 nm for AB11, AB32, and AB53, respectively, in fairly good agreement with the XRD results (Table 1). However, a close inspection of the micrographs showed that subnanoparticles were also present. In addition, particles with different geometrical shapes were found, including triangular and hexagonal particles. HRTEM studies are necessary to obtain more information on the morphology of these nickel catalysts.

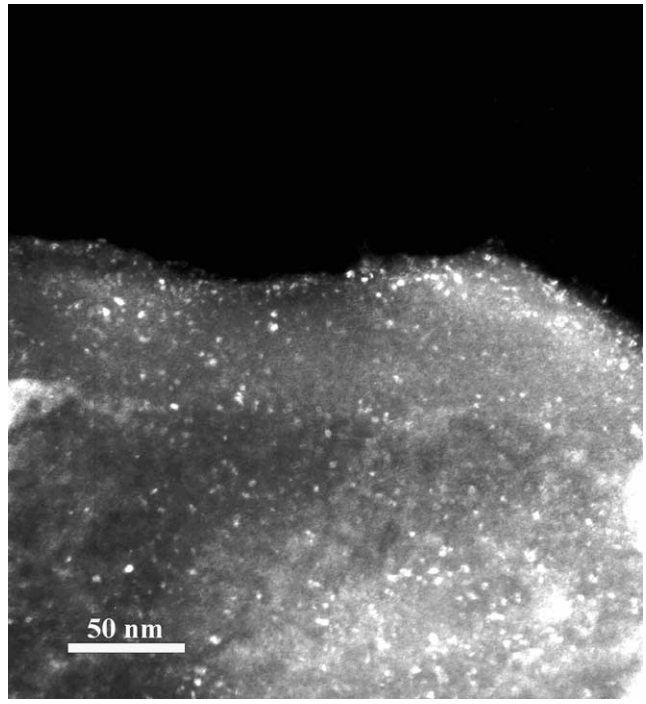

Fig. 2. TEM of fresh AB11 catalyst after H_2/300 °C treatment.

3.2. Chemisorption studies

The behavior of the silica support under hydrogen flow was first studied. It was previously treated with aqueous hydrazine and dried under the same conditions as the supported nickel catalysts. Adsorption at room temperature and H_2-TPD were performed after pretreatment under H_2 at 300 or 400 °C, using the same procedure as for the supported nickel catalysts.

The results showed that hydrazine-treated silica did not adsorb hydrogen at room temperature. However, more strikingly, the H_2-TPD study showed that some hydrogen desorbed in amounts of 4.0–6.7 $\mu mol\, g_{supp}^{-1}$. The temperature profile (Fig. 3) consisted of a main peak at 598 °C, with shoulders at 431, 502, and about 650 °C. The desorbed gas was attributed to hydrogen retained in the silica support during the thermal treatment under H_2. Earlier work showed that silica dissolved H_2 at high temperature (around 1000 °C) and the phenomenon was found to be due to the hydroxylation of silica by reduction of Si^{4+} into Si^{3+} ions resulting in the formation of a defected silica [65]. Both adsorption and desorption of hydrogen were diffusion-controlled [65]. Dissolution of hydrogen in refractory support at relatively low temperature (< 500 °C) was observed

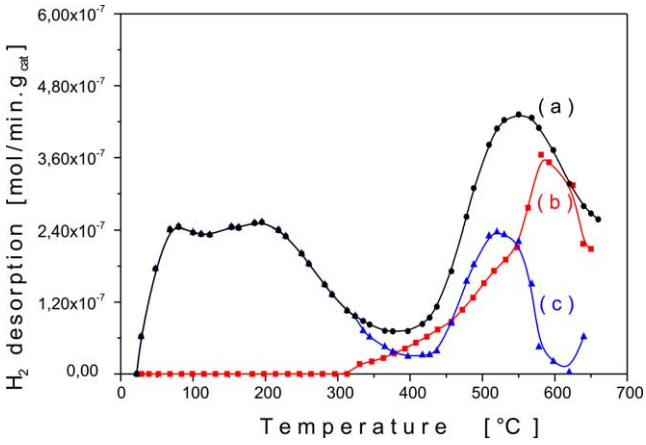

Fig. 3. H_2-TPD after treatment at H_2/400 °C/1 h followed by chemisorption of hydrogen at room temperature: (a) AB32 catalyst; (b) support; (c) subtraction.

only in the presence of a metal phase and is known as hydrogen spillover [66,67]. In the present study, the crystallized silica support may contain defects. Aqueous hydrazine or H_2 treatment at 400 °C may have activated these defects or created new ones on which hydrogen molecules or atoms strongly adsorbed. The presence of traces of metal impurities in the support may also have activated the support hydrogen adsorption.

When the support was submitted to a H_2 treatment in temperature-programmed mode, it consumed 4.0 μmol g_{supp}^{-1} of hydrogen from about 400 °C and mainly at around 600 °C. This result confirmed the hydrogen storage capability of the hydrazine-treated silica. It was also shown that a small amount of hydrogen desorbed at around 400 °C, as a result of adsorption–desorption equilibrium [68].

Classical supported nickel catalysts reduced by gaseous hydrogen give rise to H_2-TPD profiles comprising two or more reduction peaks as a result of the formation of several active sites [68]. These catalysts, as other transition-metal catalysts, are also good H_2 reservoirs, capable of adsorption and storage of large amounts of H_2 [24,64,69–72]. A similar behavior was observed for our nickel catalysts after hydrogen thermal treatment. No adsorption was observed without this treatment.

The amount of hydrogen adsorbed sharply decreased when the nickel content increased from 0.86% (AB11) to 4.3% (AB53), passing from 1506 to 252 μmol g_{Ni}^{-1} (Table 2). The metal particle sizes deduced from these values (5.5–32.8 nm) were in fair accordance with those determined by XRD and TEM (Table 1): the metallic surface increased when the nickel content decreased, as a result of an increase of metal–support interaction.

The results of Table 3 show that the amount of H_2 adsorbed by AB32 passed through a maximum pretreatment temperature of 400 °C (663 μmol g_{Ni}^{-1}). The lower amount of hydrogen adsorbed after treatment at 500 °C (271 μmol g_{Ni}^{-1}) was attributed to the sintering of the nickel phase. As to the lower amount of hydrogen adsorbed after a treatment at

Table 2
Effect nickel content on chemisorption and TPD of hydrogen after pretreatment of the catalysts under H_2/400 °C/1 h

Catalyst	H_2 uptake (μmol g_{Ni}^{-1})	H_2 desorption (μmol g_{Ni}^{-1})		
		Total	At[a] $T < T_{H_2\text{-pretreat}}$	At[a] $T > T_{H_2\text{-pretreat}}$
AB11	1506	2337	1256 (85 °C, 185 °C)[b]	1081 (510 °C)
AB12	558	1507	450 (85 °C, 185 °C)	1057 (540 °C)
AB32	663	729	326 (85 °C, 185 °C)	403 (530 °C)
AB53	252	656	165 (85 °C, 185 °C)	492 (520 °C)
AC30	286	435	183 (85 °C, 185 °C)	252 (550 °C)

[a] Desorption in the domain of temperature below or above the H_2 pretreatment temperature.

[b] Peaks of temperature at 85 and 185 °C for all catalysts. Peak of temperature.

Table 3
Chemisorption and TPD experiments on AB32 catalyst: Effect of thermal pretreatment

Pretreatment	H_2 uptake (μmol g_{Ni}^{-1})	H_2 desorption (μmol g_{Ni}^{-1})		
		Total	At[a] $T < T_{H_2\text{-pretreat}}$	At[a] $T > T_{H_2\text{-pretreat}}$
Noncalcined				
H_2/300 °C/1 h	344	414	187 (85 °C, 185 °C)[b]	227 (380 °C)
H_2/300 °C/2 h	275	527	146 (85 °C, 185 °C)	381 (400 °C)
H_2/400 °C/1 h	663	729	326 (85 °C, 185 °C)	403 (530 °C)
H_2/400 °C/2 h	553	1278	384 (85 °C, 185 °C)	894 (560 °C)
H_2/500 °C/1 h	271	707	216 (85 °C, 185 °C)	491 (650 °C)
Calcined (air/250 °C)				
H_2/300 °C/2 h	231	–	–	–
H_2/400 °C/1 h	392	714	227 (85 °C, 185 °C)	487 (580 °C)
H_2/400 °C/2 h	333	–	–	–
Calcined (air/300 °C)				
H_2/400 °C/1 h	410	733	231 (85 °C, 185 °C)	502 (570 °C)

[a,b] See Table 2.

300 °C (344 μmol g_{Ni}^{-1}), it was ascribed to the presence of the organic acetate fragment of the nickel precursor uncompletely decomposed at 300 °C [25]. The amount of hydrogen adsorbed also decreased a little (275 or 553 μmol g_{Ni}^{-1}) when the treatment time increased from 1 to 2 h. The decrease was ascribed to sintering of the metal phase with increasing time of hydrogen treatment.

The H_2-TPD profiles (Figs. 3 and 4) showed that hydrogen desorption comprised two domains of temperature. In

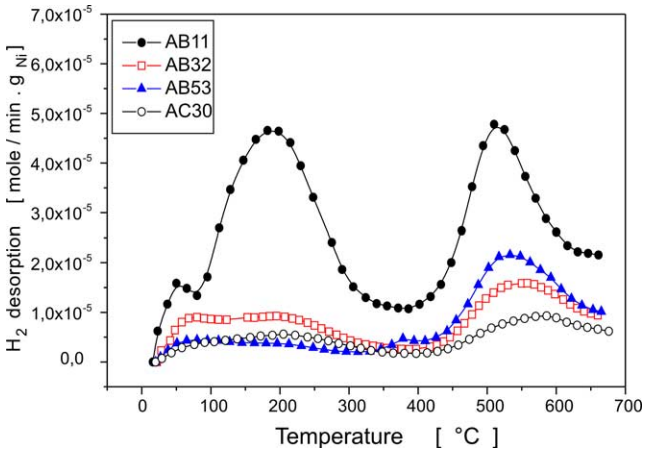

Fig. 4. H_2-TPD for the supported catalysts after H_2/400 °C/1 h treatment and chemisorption of hydrogen at room temperature.

the first domain, two large peaks more or less defined were observed with a maximum at 85 and 185 °C, respectively, for the all the catalysts. These peaks, denoted type I and I′, were ascribed to hydrogen weakly and more strongly linked to nickel active sites, respectively. In the second domain, a third peak (denoted as type II) appeared in the range 510–550 °C (Table 2) and was followed by a shoulder at higher temperatures. It was ascribed to hydrogen much more bounded to the catalyst surface. The temperature of this peak sharply increased with the temperature and of pretreatment as shown for AB32 catalysts (profile not shown). It arised at 380, 530, or 650 °C for the pretreatment temperatures of 300, 400, or 500 °C, respectively (Table 3). It slightly varied (< 30 °C) with the time of hydrogen treatment (Table 3). Moreover, the broadness of both type I–I′ and II peaks suggested the presence of small metal particles, in agreement with the XRD and TEM results (see above).

The amount of hydrogen desorbed increased from 656 to 2337 µmol g_{Ni}^{-1} when the nickel content diminished from 4.3 to 0.86% (Table 2) as a result of the increase of nickel dispersion. The small change in the amount of hydrogen desorbed between 2.73 and 4.3% Ni can be attributed to limitations in metal–support interactions as the nickel content was increased.

Table 3 shows that the amount of desorbed hydrogen by AB32 increased from 400 to about 700 µmol g_{Ni}^{-1} when the temperature of the treatment under hydrogen increased from 300 to 400–500 °C. Part of this hydrogen may have arisen from the support (Fig. 3). In addition, the increase of the hydrogen storage was mainly due to the contribution of type II hydrogen: this contribution represented 70% for the treatment at 500 °C and only 55% for the treatment at 300 or 400 °C. Since the nickel phase seemed to collapse to a certain extent at 500 °C (Table 3), the increase of the storage capacity would be ascribed to the intervention of the support, i.e., spillover hydrogen [66,67]. It is worth noting that the bare support adsorbed and desorbed hydrogen at high temperatures (Fig. 3). It was speculated that the hydrogen transfer between nickel and silica and its storage were favored at high temperatures because both the support reactivity toward hydrogen and the hydrogen diffusion rate in the silica were enhanced.

The results obtained for AB32 also show (Table 3) that, after increasing the duration of the H_2 treatment from 1 to 2 h, the amount of hydrogen desorbed increased (from 729 to 1278 µmol g_{Ni}^{-1} at 400 °C). The adsorption was mainly due to the adsorption on type II sites (70%). This is in contrast with H_2 adsorption which decreased with the time of the treatment, as a result of nickel sintering. Thus, increasing the time of hydrogen treatment also tended to sinter the active phase and enhance the hydrogen storage capacity of the catalyst, most probably through hydrogen spillover.

Submitting nickel particles inserted in an organic matrix to a previous heating in an oxidizing atmosphere before treating with hydrogen ensured a better decomposition of the organic moieties and had a beneficial effect on the surface properties of the metal phase [24,56]. In this way, fresh AB32 samples were first calcined at 250 or 300 °C, and subsequently reduced under flowing hydrogen at 300 or 400 °C. The effect of this treatment on the catalyst hydrogen chemisorption was studied.

The temperature profiles of both calcined and noncalcined catalysts were similar. Type I and type II desorption peaks were observed in both cases, suggesting similar mechanisms of the adsorption/desorption processes. However, differences appeared in the amounts of hydrogen chemisorbed according to the nature and conditions of the pretreatment, partly due to the presence of unreduced nickel particles.

The degree of reduction of the precalcined and then hydrogen-reduced catalysts was determined by chemisorption of O_2 at 400 °C [73]. They were incompletely reduced and the degree of reduction increased when the temperature or time of the hydrogen treatment increased (Table 4). These results show that the oxidized metal nanoparticles were resistant to the subsequent reducing H_2 thermal treatment, even at 400 °C. A similar behavior has been reported for classical nickel catalysts in their oxidized state, irrespective of the type of support [2–6,74]. It was accounted for by the existence of chemical interaction with the support. It has also been established that small NiO particle are less reducible than bulkier NiO, a result which has been ascribed to the low rate of nucleation in the smaller particles [6,75,76].

Furthermore, the oxygen chemisorption study showed that the fresh AB32 catalyst treated under air at 250 °C was oxidized up to 81% only (degree of reduction of 19.0%) (Table 4), in accordance with the XRD study: the small metallic particles were resistant to the oxidative treatment.

As a consequence of the presence of unreduced nickel, the calcined catalysts adsorbed less hydrogen than the noncalcined ones. Indeed, after the pretreatment with H_2/400 °C for 1 or 2 h, the calcined AB32 sample adsorbed about 40% less hydrogen than the noncalcined sample (Table 3). A second important difference between calcined and non-

Table 4
Reduction degree, TOF, and activation energy for calcined and noncalcined catalysts submitted to thermal treatment under hydrogen

Catalyst	Pretreatment	Degree of reduction (%)	Activity (175 °C) (mol min^{-1} g$_{Ni}^{-1}$)	TOF (75 °C) molec. benz. (s^{-1} site^{-1})	E_a (kJ mol^{-1})
AB11	H_2/300 °C/2 h	–	0.0362	0.030	46.3
AB12	H_2/300 °C/2 h	–	0.0210	0.031	44.9
AB32	Air 250 °C/2 h	19.0	–	–	–
	Noncalcined, H_2/300 °C/2 h	–	0.0123	0.033	46.7
	Noncalcined, H_2/400 °C/2 h	–	0.0109	0.011	46.5
	Calcined, H_2/300 °C/2 h	79.5	0.0146	0.041	45.2
	Calcined, H_2/400 °C/2 h	87.8	0.0114	0.013	51.3
	Calcined, H_2/400 °C/1 h	63.4	–	–	–
AB53	Noncalcined, H_2/300 °C/2 h	–	0.0070	0.013	46.3
AC30	H_2/300 °C/2 h	96.8	0.0050	0.010	43.5

calcined catalysts seems to reside in their behavior toward hydrogen storage: although uncompletely reduced (63.4%), the former desorbed almost the same amount of hydrogen as the noncalcined sample (714 against 729 µmol g$_{Ni}^{-1}$). In addition, it desorbed higher amount of hydrogen than it adsorbed (392 µmol g$_{Ni}^{-1}$) whereas the latter desorbed nearly the same amount of hydrogen as it adsorbed (729 against 633 µmol g$_{Ni}^{-1}$). Further, hydrogen of type II was more important in amount (70%) for the former than for the latter (55%) (Table 3). It may be concluded that the presence of oxidized nickel particles enhanced the hydrogen reservoir capacity of AB32 catalyst. Further, as far as hydrogen spillover was concerned (see above), the NiO particles were probably involved in the internal transfer of atomic or molecular hydrogen [66,67,77]. The previous oxidizing treatment may have induced specific metal–support interactions, through the formation of Ni–O–Si species, which favored the hydrogen storage [64]. Nickel in both reduced and oxidized states was found as a good hydrogen reservoir [64].

3.3. Catalytic activity

After a H_2 thermal treatment, the catalysts became active and selective in the gas-phase hydrogenation of benzene to cyclohexane. No activity was observed without this treatment. Only traces of cyclohexene and methylcyclopentane were detected. The bare silica support, previously treated in aqueous hydrazine, was inactive.

The catalysts exhibited a maximum of activity as a function of the reaction temperature (Figs. 5 and 6, Table 4). This maximum was reached around 175 °C and attributed to the competitive adsorption of the benzene and H_2 reactant molecules [24,55,56].

The catalyst with the lowest nickel content and smallest average particle size was the most efficient (Fig. 5). On the contrary, higher nickel contents (and higher average particle size) led to lower activity. These results are consistent with those of hydrogen chemisorption: the metallic surface increased with decreasing nickel content, as a result of an increasing metal–support interaction.

The effect of the H_2 pretreatment in the temperature range 200–400 °C for 1–3 h on the activity was studied in the case

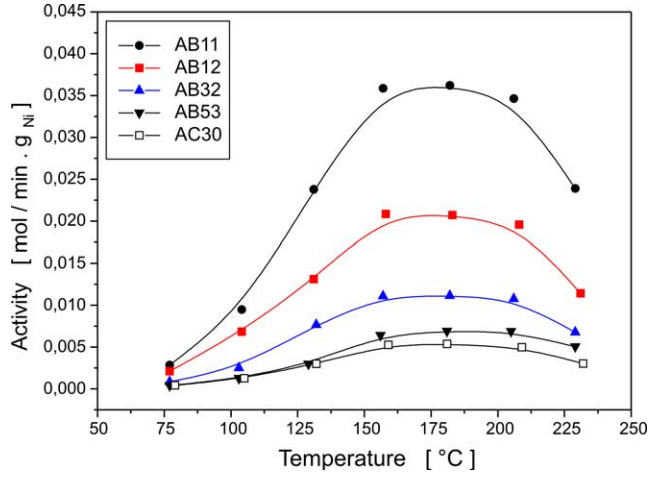

Fig. 5. Effect of nickel content on the catalytic activity. Pretreatment: H_2/300 °C/2 h.

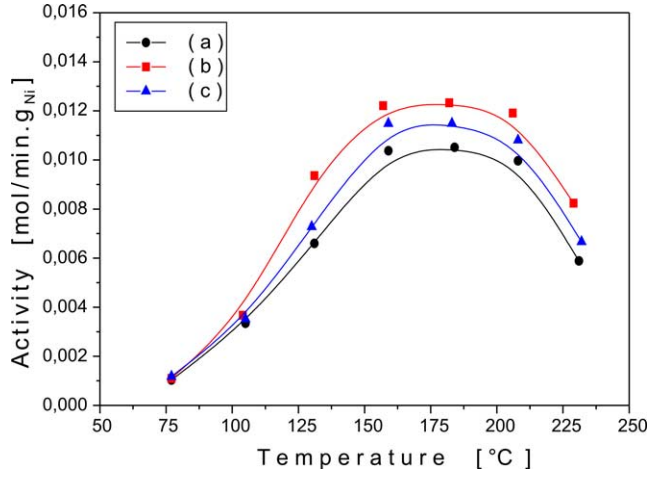

Fig. 6. Effect of hydrogen treatment time at 300 °C on the catalytic activity for the AB32-supported catalyst: (a) 1 h; (b) 2 h; (c) 3 h.

of AB32 catalyst (Table 4, Fig. 6). The best activity was obtained for the treatment temperature and time of 300 °C and 2 h, respectively: at the maximum of conversion, the specific activity was 12.3×10^{-3} mol min^{-1} g$_{Ni}^{-1}$. These conditions, as suggested for the chemisorption results (Table 3), are a

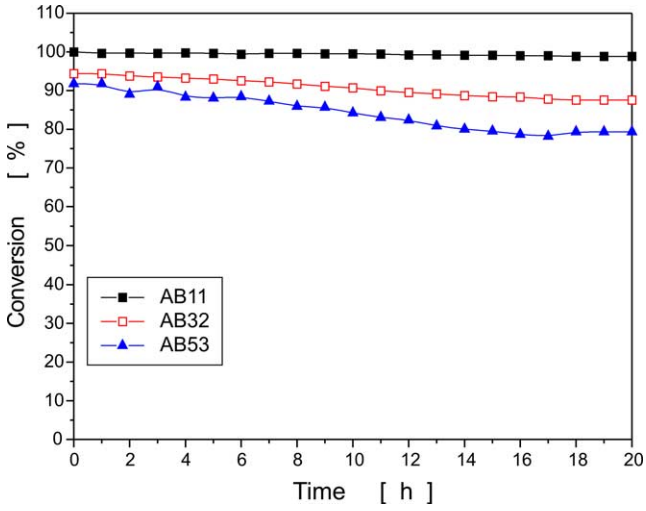

Fig. 7. Conversion versus time on stream at 175 °C.

good compromise between the removal of the organic matrix and the sintering of the metal particles.

The stability of the catalysts was tested by crossing the reaction temperature (see Experimental). The obtained curves (see Figs. 5 and 6) showed almost no deactivation. Notably, the initial activity at 75 °C was almost totally recovered at the end of each run. However, for longer working time, some deactivation was observed in the high conversion regime (> 80%) for high nickel contents only (Fig. 7). It was concluded that the lower the nickel content, the smaller the nickel particle size and the better the stability of the catalyst.

The turnover frequencies (TOFs) for the reaction temperature of 75 °C (< 10% of conversion) are given in Table 4. The results obtained (0.011–0.033 s^{-1}) are in fair agreement with the reported values obtained at 80 °C over classical Ni/SiO_2 catalysts (0.005–0.025 s^{-1}) [74]. On the other hand, benzene hydrogenation appeared as structure insensitive under our conditions. Indeed, it is generally accepted that reactions are structure sensitive when TOF variation vs particle size is much higher than 3 for metal particle size below 3–5 nm [58–60,74]. In the present case, e.g., the TOF was divided by 3.0 (Table 4) when the chemisorbed hydrogen amount was multiplied by 2.0 (Table 3). The values of both the TOF gap ($\leqslant 3$) and metal particle size used (around 10 nm) are not in the range of that required for structure-sensitive reactions. Structure sensitivity of benzene hydrogenation on nickel catalysts is still an open question [56–59,76,78,79].

The activation energy, of about 47.0 kJ mol^{-1} in the temperature range 75–150 °C, is in good agreement with that reported in the literature for classical nickel catalysts (50.0–58.0 kJ mol^{-1}) [56,58].

The effect of previous oxidizing treatment on the catalytic properties of the nickel nanoparticles was examined. The results reported in Table 4 show that, as for the noncalcined catalyst, the activity of the calcined catalyst was not correlated to the metal surface area: e.g., the TOF was divided by 3.1 (Table 4) when that of chemisorbed hydrogen amount was multiplied by 1.4 (Table 3). However, the calcined catalyst appeared to be more active than the noncalcined catalyst since, for the same temperature of hydrogen treatment, the TOF was higher: +24% (H_2/300 °C/2 h) or +18% (H_2/400 °C/2 h) (Table 4). Such a change in the behavior of the nickel nanoparticles may be related to the presence of unreduced nickel in the calcined catalyst [56,64,80,81]. The previous oxidizing treatment may also have induced specific Ni–O–Si interactions which enhanced the activation of the reactant molecules [56,64,80]. Certain authors believe that unreduced nickel decreased the size of the nickel particles required for the adsorption of benzene in a planar mode [80].

The activation energy was 45.2 or 51.3 kJ mol^{-1}, a value in good agreement with those observed for the noncalcined catalysts. The similar activation energy for both types of catalysts indicates that the presence of unreduced nickel did not change the reaction mechanism of the gas-phase hydrogenation of benzene.

3.4. Conventional catalyst properties

The results obtained for the classical AC30 catalyst are reported in Tables 1, 2, and 4 and Figs. 4 and 5. They were compared to that of the AB53 catalyst which had a similar nickel content (around 4.5%).

The conventional catalyst adsorbed almost the same amount (286 µmol g_{Ni}^{-1}) of hydrogen as the AB53 catalyst (252 µmol g_{Ni}^{-1}) (Table 2), and had a similar metal particle size (Table 1). On the other hand, both catalysts exhibited similar TPD profiles (Fig. 4): type I and II peaks were observed for both solids at nearly the same temperatures. However, the conventional catalyst stored about 30% less hydrogen than the nonclassical catalyst (Table 2). In addition, the contribution of type II sites to the hydrogen storage was less important (57.9%) for AC30 than for AB53 (75.0%) (Table 2). These sites seemed to have been favored by the hydrazine reductor during the preparation step.

The AC30 catalyst was active and selective in benzene hydrogenation. It behaved similarly as the nonclassical catalyst in this reaction: a maximum of activity was observed at 175 °C and the activation energy was 43.5 kJ mol^{-1} (Table 4). However, it was less active than the AB53 catalyst: the maximum of conversion reached 85% only against 96% for AB53. The TOFs were also less important: 0.010 s^{-1} against 0.013 s^{-1} for AB53, that is 1.3 time lower. The hydrazine reduction method seemed to be more efficient in the preparation of active supported nickel catalyst.

4. Conclusions

Nickel metallic nanoparticles obtained by reduction of nickel acetate by hydrazine in aqueous medium and supported on a low surface area silica have been investigated. The support was involved in the reduction process. The

XRD, TEM, and hydrogen adsorption studies showed that the mean size of the fresh particles increased under H_2 flow, and all the more as the temperature and treatment time increased. Small metal particles were resistant to oxidative thermal treatment which, in addition, decreased their mean size. Conversely, previously calcined particles under air/250 °C were resistant to reduction under H_2 flow at 300–500 °C.

The TPD profiles of hydrogen exhibited two domains of temperature. The first domain consisted of two desorption peaks at 85 and 180 °C (denoted type I and I′) ascribed to hydrogen weakly and strongly linked to active nickel sites, respectively. This domain did not depend on the temperature of pretreatment. In the second domain, a large peak (denoted type II) appeared at a temperature and with an area increasing with the temperature and time of pretreatment. This peak was ascribed to hydrogen much more strongly bounded to the catalyst surface. The bare support also adsorbed a nonnegligible amount of hydrogen and exhibited a desorption peak at a temperature similar to the type II peak. The TPD results strongly suggested the occurrence of spillover hydrogen from the nickel phase onto the silica support. Unreduced nickel also seemed to be involved in hydrogen spillover in the case of the precalcined catalysts.

The supported nickel nanoparticles exhibited high activity in benzene hydrogenation provided the organic fragment of the metal precursor was decomposed under hydrogen or air at moderate temperature. High temperature and longer time of reduction depressed the catalyst efficiency as a result of the nickel sintering. The TOFs for the calcined catalyst were 18–24% higher than for the noncalcined catalyst, and correlated with the presence of unreduced nickel phase.

A comparative study showed that the supported nickel catalyst prepared by reduction with aqueous hydrazine stored more hydrogen and was more active in benzene hydrogenation than a conventional Ni catalyst. The TOFs were 1.3 times higher.

References

[1] T.S. Armadi, Z.L. Wang, T.C. Green, A. Heinglein, M.A. El-Sayed, Science 272 (1996) 1924.
[2] S.J. Tautster, S.C. Fung, J. Catal. 5 (1978) 29.
[3] C.H. Bartholomew, Mustard, J. Catal. 67 (1981) 186.
[4] J. Zelinski, J. Catal. 76 (1982) 157.
[5] J.T. Richardson, M. Lei, B. Turk, K. Forster, M.V. Twigg, Appl. Catal. 110 (1994) 217.
[6] R. Molina, G. Poncelet, J. Catal. 173 (1998) 257.
[7] A. Miyazaki, I. Balin, K. Aika, Y. Nakano, J. Catal. 204 (2001) 364.
[8] D. Reinen, P.W. Selwood, J. Catal. 2 (1963) 109.
[9] M. Houalla, J. Lemaître, B. Delmon, J. Chem. Soc., Faraday Trans. 78 (1982) 1389.
[10] G.R. Gavallas, C. Phishitkul, G.E. Voecks, J. Catal. 88 (1984) 54.
[11] W.P. Halperin, Rev. Mod. Phys. 58 (1998) 533.
[12] G. Schmid, Chem. Rev. 92 (1992) 1709.
[13] J.S. Bradley, E.W. Will, C. Klein, B. Chaudret, A. Duteil, Chem. Mater. 5 (1993) 2540.
[14] H. Hirai, Y. Nakao, N. Toshima, J. Macromol. Sci. Chem. A 13 (1979) 727.
[15] L.N. Lewis, Chem. Rev. 93 (1993) 2693.
[16] Y. Volotkin, J. Sinzig, L.J. De Jong, G. Schmid, M.N. Vargaftik, I.I. Moisseev, Nature 384 (1996) 621.
[17] V.N. Colvin, M.C. Schlamp, A.P. Alivisatos, Nature 370 (1994) 354.
[18] R.L. Whetten, Acc. Chem. Res. 32 (1999) 397.
[19] B.C. Gates, Chem. Rev. 95 (1995) 511.
[20] R. Brayner, G. Viau, F. Bozon-Verduraz, J. Mol. Catal. A 182–183 (2002) 227.
[21] U.A. Paulus, U. Endrushchat, G.J. Feldmeyer, T.J. Schmidt, H. Bonnemann, R.J. Behm, J. Catal. 195 (2000) 383.
[22] W. Yu, H. Liu, X. Ma, Z. Liu, J. Colloid Interface Sci. 208 (1998) 439.
[23] E.A. Sales, B. Benhamida, V. Caizergues, J.P. Lagier, F. Fievet, F. Bozon-Verduraz, Appl. Catal. 172 (1998) 273.
[24] D. Franquin, S. Monteverdi, S. Molina, M.M. Bettahar, Y. Fort, J. Mater. Sci. 34 (1999) 4481.
[25] S. Lefondeur, S. Monteverdi, S. Molina, M.M. Bettahar, Y. Fort, J. Mater. Sci. 36 (2001) 2633.
[26] L.K. Kurihara, G.M. Chow, P.E. Shoen, Nanostruct. Mater. 5 (1995) 607.
[27] T.D. Xiao, S. Torban, P.R. Strut, B.H. Kear, Nanostruct. Mater. 7 (1996) 857.
[28] J.H. Fendler, F.C. Meldrum, Adv. Mater. 7 (1995) 607.
[29] F. Fievet, F. Fievet-Vincent, J.P. Lagier, B. Dumont, M. Figlarz, J. Mater. Chem. 3 (1993) 627.
[30] R.D. Rieke, Acc. Chem. Res. 10 (1997) 377.
[31] R.D. Rieke, Science 246 (1989) 1260.
[32] G.A. Ozin, Adv. Mater. 4 (1992) 612.
[33] G.N. Glavee, Inorg. Chem. 32 (1993) 474.
[34] H. Bonnemain, W. Brijoux, T. Joussen, Angew. Chem., Int. Ed. Engl. 29 (1990) 273.
[35] D. Zeng, M.J. Hampten-Smith, Chem. Mater. 5 (1993) 68.
[36] K. Vijaya Sarathy, G.U. Kulkarny, C.N.R. Rao, Chem. Commun. (1997) 537.
[37] P. Gallezot, C. Leclercq, Y. Fort, P. Caubere, J. Mol. Catal. 93 (1994) 79.
[38] J.J. Brunet, P. Gallois, P. Caubere, J. Org. Chem. 45 (1980) 1937.
[39] N. Toshima, Y. Wang, Adv. Mater. 6 (1994) 245.
[40] A. Heinglein, J. Phys. Chem. 97 (1993) 5457.
[41] J.S. Bradley, J.M. Millar, E.W. Hill, S. Behal, B. Chaudret, Faraday Discuss. 92 (1991) 255.
[42] J.C. Poulin, H.B. Kagan, M.N. Vargavtik, I.P. Stolarov, I.I. Moisseev, J. Mol. Catal. 95 (1995) 109.
[43] C. Amiens, D. de Caro, B. Chaudret, J.S. Bradley, R. Mazel, C. Roucau, J. Am. Chem. Soc. 115 (1993) 11638.
[44] N. Toshima, T. Takahashi, Bull. Chem. Soc. Jpn. 65 (1992) 400.
[45] K. Esumi, K. Matzuhita, K. Torigoe, Langmuir 11 (1995) 3285.
[46] D.V. Leff, P.C. Ohara, J.R. Heath, W.M. Gelbart, J. Phys. Chem. 99 (1995) 7036.
[47] H. Bönnemann, W. Brijoux, R. Brinkmann, E. Dinjus, E. Joussen, B. Korall, Angew. Chem., Int. Ed. Engl. 30 (1991) 1312.
[48] M.T. Reetz, W. Helbig, J. Am. Chem. Soc. 116 (1994) 7401.
[49] N. Toshima, T. Teranishi, H. Asanuma, Y. Saito, J. Phys. Chem. 96 (1992) 3796.
[50] S.J. Tauster, Acc. Chem. Res. 20 (1987) 389.
[51] R. Brayner, G. Viau, G.M. da Cruz, F. Fiévet-Vincent, F. Fiévet, F. Bozon-Verduraz, Catal. Today 57 (2000) 187.
[52] J.L. Pellegatta, C. Blandy, V. Collière, R. Choukroun, B. Chaudret, P. Cheng, K. Phillipot, J. Mol. Catal. A 178 (2002) 55.
[53] A. Stanislaus, B.H. Cooper, Catal. Rev. Sci. Eng. 36 (1994) 75.
[54] K. Weissermel, H.J. Arple, Industral Organic Chemistry, 3rd ed., VCH, New York, 1997.
[55] M.A. Keane, J. Catal. 166 (1997) 347.
[56] R. Molina, G. Poncelet, J. Catal. 199 (2001) 162.
[57] B. Coughlan, M.A. Keane, Zeolites 11 (1991) 12.

[58] K.J. Yoon, M.A. Vannice, J. Catal. 82 (1983) 457.
[59] L. Daza, B. Pawelec, J.A. Anderson, J.L.G. Fierro, Appl. Catal. 87 (1992) 145.
[60] R. Burch, R. Flambard, J. Catal. 85 (1984) 16.
[61] A. Bensalem, G. Shafeev, F. Bozon-Verduraz, Catal. Lett. 18 (1993) 165.
[62] Y.D. Li, L.Q. Li, H.W. Liao, H.R. Wang, J. Mater. Chem. 9 (1999) 2675.
[63] L.M. Bronstein, O.A. Platonova, A.N. Yakunin, I.M. Yanovskaya, P.M. Valetsky, A.T. Dembo, E.S. Obolonkova, E.E. Makhaeva, A.V. Mironov, A.R. Khokhlov, Colloid Surf. 147 (1999) 221.
[64] M.P. Sohier, G. Wröbel, J.P. Bonnelle, J.P. Marq, Appl. Catal. A 84 (1992) 169.
[65] P. Pascal, in: Nouveau Traité de Chimie Minerale, vol. VIII, Masson, Paris, 1965, p. 93.
[66] S.T. Srinivas, P. Kanta Rao, J. Catal. 148 (1994) 470.
[67] J.L. Carter, in: Proceedings, 3rd International Congress on Catalysis, Amsterdam, vol. 1964, Wiley, New York, 1965, p. 1.
[68] J.J.F. Sholten, A.P. Pijpers, A.M.L. Hustings, Catal. Rev. Sci. Eng. 27 (1985) 151.
[69] L. Jalowiecki, G. Wröbel, M. Daage, J.P. Bonnelle, J. Catal. 107 (1987) 375.
[70] D. Duprez, J. Barbier, Z. Ferhat-Hamida, M.M. Bettahar, Appl. Catal. 12 (1984) 219.
[71] G. Wröbel, L. Jalowiecki, J.P. Bonnelle, F. Bali, M.M. Bettahar, New J. Chem. 11 (1987) 715.
[72] Z. Mesbah-Benyoucef, M.M. Bettahar, J. Barrault, A. Tranchant, R. Messina, C_1 Mol. Chem. 2 (1987) 33.
[73] C.H. Bartholomew, R.J. Farrauto, J. Catal. 45 (1976) 41.
[74] M. Houalla, F. Delannay, B. Delmon, J. Chem. Soc., Faraday Trans. 76 (1980) 2128.
[75] C.H. Li, Y.W. Chen, Thermochim. Acta 256 (1995) 457.
[76] M. Boudart, Adv. Catal. 20 (1969) 153.
[77] T. Takeguchi, S. Furukawa, M. Inoue, J. Catal. 202 (2001) 14.
[78] R.Z.C. van Meerten, A. Morales, J. Barbier, R. Maurel, J. Catal. 58 (1979) 493.
[79] M. Che, C.O. Bennett, Adv. Catal. 36 (1989) 55.
[80] J.A. Anderson, L. Daza, J.L. Fierro, T. Rodrigo, J. Chem. Soc., Faraday Trans. 89 (1993) 3651.
[81] J.A. Anderson, L. Daza, S. Damayanova, J.L. Fierro, T. Rodrigo, Appl. Catal. 113 (1994) 75.